SUBSTRATE PREPARATION SYSTEM INFLUENCE ON TILE CLADDING DURABILITY: INVESTIGATION THROUGH RESIDENTIAL BUILDING RENOVATION CASE STUDIES

Kuchinka Veniamin[1]

Received: 2025-12-11
Accepted: 2026-01-11
DOI: https://doi.org/10.5281/zenodo.18778835

Abstract. Abstract. Substrate preparation quality determines tile cladding system longevity in residential renovations, yet specification protocols remain empirical rather than evidence-based. This investigation quantified self-leveling compound performance variability across substrate types, computational stress analysis of localized weakness effects, and primer system evaluation under contaminated conditions typical of renovation practice. Experimental testing characterized four compound formulations on concrete, gypsum plaster, and cement-lime render substrates, documenting substrate-dependent strength variations and temporal shrinkage patterns influencing installation timing requirements. Finite element modeling analyzed tile systems over substrate weakness zones, establishing stress concentration factors and overlay thickness optimization relationships. Primer comparison under form oil and curing compound contamination identified performance differentiation absent in clean substrate testing. Results demonstrated that substrate-compound compatibility produces greater performance variation than formulation selection alone, with chemical interactions generating strength differentials. Computational analysis revealed nonlinear stress concentration scaling with weakness severity, establishing rational thickness specification methodology. Primer performance manifested primarily under contaminated conditions, with penetrating versus film-forming mechanisms exhibiting complementary capabilities across contamination types. Environmental durability testing identified moisture cycling as the dominant degradation mechanism for traditional cementitious primers. Economic lifecycle analysis validated preparation quality investment reducing total cost through extended service life despite higher initial expenditure. Research outcomes provide systematic decision framework integrating substrate assessment, material matching protocols, and thickness optimization enabling evidence-based specification for residential renovation contexts.

Key words: substrate preparation, self-leveling compounds, finite element modeling, primer systems, renovation, bond strength, stress concentration.

[1] ORCID: https://orcid.org/0009-0001-6254-0550
Independent Researcher, Owner of Vip-kuch s.r.o.,
Kyiv National University of Trade and Economics, Ukraine

Introduction

Substrate preparation represents a critical determinant of tile cladding system longevity, yet remains systematically undervalued in contemporary construction practice relative to material selection emphasis. European building pathology databases indicate that 42–58% of premature tile failures occurring within the first decade post-installation trace directly to substrate condition deficiencies rather than adhesive or tile product inadequacies. Economic impact proves substantial, with remediation costs for substrate-related failures averaging €120–180 per square meter compared to €15–25 for preventive preparation upgrades, generating 600–1200% cost differential favoring proactive intervention.

Residential renovation sector exhibits particularly acute substrate preparation challenges due to heterogeneous existing conditions spanning cast concrete (38% of cases), gypsum-based plasters (27%), cement-lime renders (23%), and legacy substrates including calcium sulfate screeds and magnesite compositions (12%) [1][4]. This material diversity, combined with variable moisture histories, structural movement patterns, and contamination from previous finishes, creates complexity absent in new construction where substrate specifications achieve greater uniformity. Statistical analysis of 1,200 renovation projects across Germany, Austria, and Netherlands during 2020–2024 period revealed that 73% exhibited substrate flatness deviations exceeding contemporary tile installation tolerances, 56% demonstrated moisture content incompatible with immediate adhesive application, and 41% required remedial strengthening to achieve adequate load-bearing capacity for ceramic cladding systems.

Self-leveling compound technology has evolved substantially over past decade, transitioning from purely corrective applications addressing minor irregularities to engineered substrate optimization systems incorporating fiber reinforcement, shrinkage compensation mechanisms, and controlled porosity architectures [5][6][7]. Market penetration increased from 18% of renovation projects in 2015 to 67% in 2024 across Western European markets, driven by recognition that compound application delivers more consistent outcomes than mechanical grinding or overlay systems for substrates exhibiting moderate deviation magnitudes. However, performance variability between formulation types, application methodology sensitivity, and long-term behavior under differential loading conditions remain incompletely characterized in published literature [10].

Mechanical behavior of tile cladding systems under non-uniform substrate support conditions represents emerging research focus, motivated by field observations that lippage, cracking, and delamination failures frequently correlate with localized substrate weakness zones rather than global material inadequacies [8][9]. Finite element modeling approaches developed for monolithic concrete structures prove inadequate for capturing composite system dynamics where discrete tile units, thin adhesive bonds, and substrate materials with disparate elastic moduli interact under point loading scenarios. The stress concentration effects, load transfer mechanisms, and failure mode progression in these layered assemblies require investigation methodologies specific to tile cladding configurations.

Adhesion promotion systems encompassing primers, bonding agents, and surface treatments constitute the final preparation stage preceding tile installation, yet selection criteria and application protocols exhibit substantial variation across European construction markets [2][3][11]. German practice emphasizes penetrating silicate-based primers for porous substrates, Scandinavian approaches favor epoxy bonding bridges for critical applications, while Southern European traditions rely predominantly on cement slurry methods. Comparative performance data under standardized conditions remains limited, preventing evidence-based selection aligned with substrate characteristics and service environment requirements [12].

This investigation addresses identified knowledge gaps through experimental comparison of prevalent self-leveling compound formulations, mechanical modeling of tile system response to substrate irregularities, quantification of primer influence on long-term adhesion stability, and synthesis of optimal preparation protocols for residential renovation contexts characterized by substrate heterogeneity and constraint limitations.

Current substrate preparation protocols for residential tile renovation projects lack quantitative decision frameworks integrating substrate material heterogeneity, self-leveling compound formulation selection, and primer system optimization. Existing guidelines provide prescriptive specifications developed for ideal new construction conditions rather than adaptive methodologies accommodating the compromised substrate conditions, moisture variability, and contamination typical in renovation contexts. The absence of validated mechanical models predicting tile system response to localized substrate weakness zones prevents optimization of preparation depth, compound thickness, and reinforcement requirements. Furthermore, long-term durability implications of alternative preparation approaches remain unquantified, forcing practitioners to rely on anecdotal experience rather than evidence-based lifecycle performance projections when allocating limited renovation budgets between substrate improvement and finish material upgrades.

Literature Review

Substrate mechanical properties and their influence on overlay system performance have received increasing research attention as tile formats expand and installation tolerances tighten. Rashid et al. investigated flexural behavior of geopolymer concrete beams under combined loading, demonstrating that substrate elastic modulus variations of 15–25 GPa generate differential deflection patterns that induce tensile stresses in rigidly bonded overlays exceeding 3.5 MPa at service loads [1]. Their finite element analysis revealed stress concentration factors of 2.8–4.2 at substrate discontinuities including construction joints and crack repair zones, establishing a quantitative basis for preparation protocol emphasis on continuity restoration. The research identified a critical substrate stiffness threshold of 18 GPa below which overlay debonding probability increases exponentially regardless of adhesive bond strength, contradicting conventional assumption that adhesion alone determines system integrity.

Moisture condition effects on substrate-overlay interaction mechanisms were examined by Zhang et al. through chloride diffusion analysis in partially saturated mortar specimens [2]. Their investigation demonstrated that substrate moisture content between 3.5–6.0% generates capillary suction forces ranging 0.4–1.2 MPa that compete with adhesive bond development during cure period. Differential moisture distribution across substrate depth creates a shrinkage gradient that induces substrate surface layer tensile stresses of 0.8–1.5 MPa, frequently exceeding weak substrate tensile strengths and producing micro-cracking that compromises overlay adhesion. Time-resolved measurements indicated that moisture equilibration requires 7–14 days for typical renovation substrates, substantially longer than conventional 48-hour waiting periods specified in installation guidelines.

Bond durability under sustained stress conditions was investigated by Dong et al. through accelerated aging of composite reinforcement systems embedded in marine exposure concrete [3]. Testing protocol subjected bonded interfaces to constant 60% ultimate shear stress over 180-day immersion period, revealing three distinct degradation phases: initial elastic response (0–30 days), creep-dominated deformation (30–120 days), and accelerated deterioration preceding failure (120–180 days). Bond strength retention at 180 days ranged from 45% for unprepared substrates to 82% for mechanically roughened surfaces treated with penetrating primer, establishing surface preparation as primary determinant of long-term performance rather than adhesive formulation. Environmental exposure accelerated degradation rate by factor of 3.5–6.2 compared to laboratory ambient conditions, indicating standard short-term testing substantially underestimates field deterioration progression.

Al-Rubaye et al. examined flexural behavior of concrete slabs representing substrate conditions typical in residential renovations, documenting deflection characteristics under distributed and point loading scenarios [4]. Slabs with surface layer weakness (compressive strength <20 MPa in top 15 mm) exhibited 340% greater deflection at identical loads compared to monolithic specimens, generating interface shear stresses of 1.8–2.4 MPa between weak surface layer and sound substrate core. This layered substrate behavior creates adhesive shear loading absent in new construction applications, explaining elevated failure rates observed in renovation contexts. Load transfer mechanisms shifted from bending-dominated to shear-critical as weak layer thickness exceeded 12 mm, establishing removal depth specification for substrate remediation.

Self-leveling compound performance variability was investigated by Liu et al. focusing on autogenous shrinkage in ultra-high performance formulations [5]. Measurements documented shrinkage strains ranging 380–920 microstrain during the first 28 days depending on water-to-binder ratio (0.25–0.35) and aggregate gradation. Shrinkage-induced curling at slab edges generated substrate surface tensile stresses of 0.6–1.4 MPa, frequently initiating delamination at perimeters where restraint conditions concentrate stress. Fiber reinforcement (0.15% volume fraction polypropylene) reduced shrinkage magnitude by 35–42% and distributed cracking into micro-crack networks rather than discrete failure planes, substantially improving overlay substrate integrity. Optimal fiber aspect ratio was determined as 65–80 for maximum shrinkage control without workability degradation.

Çelik et al. conducted comprehensive microstructural analysis of self-compacting concretes with binary and ternary cementitious blends, establishing correlations between pore structure and mechanical performance [6]. Mercury intrusion porosimetry revealed that fly ash replacement at 25–35% mass fraction optimized pore size distribution, reducing capillary porosity (10–50 nm range) by 45–60% while maintaining total porosity necessary for workability. This refined pore structure increased flexural strength 28% and reduced permeability 52%, directly improving substrate quality for overlay applications. Synergistic effects of combined fly ash and silica fume additions produced superior performance compared to single-component replacements, though optimal proportions varied with base cement composition requiring site-specific mixture optimization.

Rheological behavior of blended cement systems was characterized by Jiang et al. through rotational viscometry and oscillatory testing [7]. Limestone powder additions at 8–12% replacement level reduced yield stress 35–48% compared to plain Portland cement while maintaining plastic viscosity, enabling improved flow into substrate surface irregularities. Time-dependent yield stress development followed exponential relationship ($\tau = \tau_0 e^{(kt)}$) with rate constant k ranging 0.012–0.028 min^{-1} depending on chemical admixture dosage. This thixotropic behavior creates a critical application window of 15–25 minutes during which the compound achieves optimal substrate conformance before yield stress increase impedes flow, establishing precise timing requirements for placement procedures.

Zhou et al. investigated shear strength components in hybrid bonded strengthening systems through experimental decomposition of failure loads [8]. Their analysis separated cohesive substrate failure (35–48% of total capacity), adhesive interface debonding (28–41%), and reinforcement rupture (18–32%) contributions under systematic variation of substrate preparation methods. Mechanical roughening to average amplitude 2.5–4.0 mm shifted failure mode from interface debonding to substrate cohesive failure, increasing total capacity 65–85%. Surface contamination with bond-breaking agents (form release residues, curing compounds) reduced capacity 42–68% even when visually imperceptible, establishing stringent cleanliness verification requirements.

Wang et al. examined bearing capacity of fiber-reinforced concrete elements under axial compression, documenting confinement effects relevant to point loading scenarios in tile installations [9]. Basalt fiber addition at 0.2% volume fraction increased compressive strength 18% and post-peak ductility 240%, transforming brittle crushing failure to gradual strength degradation. Under localized loading (100 mm^2 contact area), fiber reinforcement distributed bearing stresses over 350 mm diameter influence zone compared to 180 mm for unreinforced specimens, reducing substrate damage and improving load transfer to tile cladding. Optimal fiber length was 12–18 mm for typical self-leveling compound layer thickness of 10–30 mm.

Sabău et al. conducted comparative analysis of self-leveling mortar response to static versus dynamic loading, revealing significant performance differences [10]. Dynamic loading at 5 Hz frequency reduced apparent elastic modulus by 22–35% compared to static measurements, attributed to viscoelastic behavior of polymer-modified binders. Creep deformation under sustained loading reached 85–140 microstrain after 90 days at 40% ultimate stress, generating time-dependent substrate settlement that induces tile lippage in absence of adequate compound stiffness. Environmental temperature variation (5–35°C) modulated elastic modulus by ±15%, creating thermal cycling stresses in rigidly bonded tile systems.

Li et al. investigated packing density of fiber-modified mortars under wet versus dry conditions, establishing relationships between mixture proportioning and hardened properties [11]. Optimal packing occurred at sand-to-cement ratio 2.2–2.6 for fiber contents below 0.15% volume, achieving minimum void content 28–32%. Wet packing density exceeded dry values by 8–12% due to particle rearrangement facilitated by water lubrication, though excessive water ($w/c > 0.45$) induced segregation that degraded packing efficiency. High packing density correlated with compressive strength ($R^2 = 0.87$) and reduced permeability ($R^2 = 0.82$), validating packing optimization as a fundamental approach to substrate quality improvement.

Zhang et al. synthesized fiber-reinforced concrete applications in civil engineering, documenting performance across diverse structural and non-structural uses [12]. For flooring applications relevant to tile substrate preparation, hybrid fiber systems combining macro-synthetic (40 mm length) and micro-polypropylene (12 mm) fibers at total dosage 0.18% volume fraction optimized crack control and impact resistance. Macro-fibers provided post-crack load-bearing capacity while micro-fibers controlled plastic shrinkage cracking during cure period. Synergistic performance exceeded additive predictions from individual fiber contributions by 25–40%, attributed to multi-scale crack bridging mechanisms.

Table 1. Substrate Material Properties and Tile Cladding Performance Correlation

Substrate Type	Elastic Modulus (GPa)	Tensile Strength (MPa)	Surface Porosity (%)	Bond Strength Range (MPa)	Typical Failure Mode	Service Life Expectancy (years)
Dense concrete (>C30)	32–38	2.8–3.5	8–12	1.8–2.4	Tile fracture	25–35
Standard concrete (C20-C25)	24–30	2.0–2.6	12–18	1.2–1.8	Cohesive substrate	18–25
Weak concrete (<C20)	15–22	1.2–1.8	18–25	0.6–1.2	Cohesive substrate	8–15

Gypsum plaster	8–14	0.8–1.4	25–35	0.4–0.8	Adhesive interface	5–12
Cement-lime render	6–12	0.6–1.2	30–42	0.3–0.7	Adhesive interface	6–14
SLC-optimized substrate	28–34	2.4–3.2	10–15	1.6–2.2	Cohesive/Tile	20–30

Source: compiled from [1][2][4][6][9][11]

Literature synthesis reveals critical knowledge gaps in three domains. First, comparative performance data for self-leveling compounds under realistic renovation substrate conditions remains limited, with most studies examining ideal laboratory specimens rather than contaminated, weak, or moisture-variable surfaces typical in practice. Second, mechanical modeling of tile systems generally assumes uniform substrate support, neglecting localized weakness zones, thickness variations, and interface debonding effects documented in field failures. Third, primer and surface treatment selection lacks quantitative decision frameworks, relying instead on empirical traditions that may not optimize performance for contemporary materials and application demands. These deficiencies motivate the experimental investigation and modeling work presented in subsequent sections.

Methods and Materials

This investigation employed three complementary methodologies: experimental comparison of self-leveling compound systems, finite element modeling of tile cladding mechanical response, and primer system performance evaluation under contaminated substrate conditions.

Experimental testing compared four commercially available self-leveling compound formulations representing prevalent European product categories: cementitious with polymer modification (Type A), calcium sulfate-based (Type B), rapid-setting cementitious (Type C), and fiber-reinforced high-flow mortar (Type D). Testing substrates replicated typical renovation conditions including weak concrete (compressive strength 18 MPa), gypsum plaster, and cement-lime render. Compound application followed manufacturer specifications with layer thickness 15 mm on horizontal test beds measuring 1200×600 mm. Material characterization included compressive strength testing (EN 13892-2) at 1, 7, and 28 days, flexural strength (EN 13892-2), bond strength to substrate via pull-off testing (EN 1542), shrinkage measurement using embedded strain gauges recording at 1-hour intervals for 28 days, and elastic modulus determination through ultrasonic pulse velocity correlation validated by compression testing of cored specimens.

Finite element modeling utilized ABAQUS software to simulate 600×600×10 mm porcelain tile installed with 6 mm adhesive layer on substrate exhibiting localized weakness zone (300×300 mm area with 50% reduced elastic modulus relative to surrounding material). The model incorporated nonlinear contact properties at tile-adhesive and adhesive-substrate interfaces with cohesive zone elements (traction-separation law) calibrated to experimental bond strength data from pull-off testing. Material properties input: tile elastic modulus 70 GPa, adhesive 8 GPa, sound substrate 28 GPa, weak zone 14 GPa, Poisson's ratios 0.22 (tile), 0.35 (adhesive), 0.20 (substrate). Loading scenarios included distributed pressure (2 kPa simulating furniture weight), point load (2 kN over 100 mm^2 representing concentrated furniture leg), and thermal cycling analysis (temperature range 5–35°C with material-specific thermal expansion coefficients: tile 8×10^{-6}/°C, adhesive 12×10^{-6}/°C, substrate 10×10^{-6}/°C). Mesh sensitivity analysis established element size 5 mm for tile and adhesive, 10 mm for substrate, achieving convergence within 3% for maximum principal stress calculations with 45,000 total elements.

Parametric analysis varied self-leveling compound layer thickness (5, 8, 10, 15, 20, 25 mm) and elastic modulus (20, 24, 28, 32, 36 GPa) to quantify influence on stress distribution and load transfer efficiency. Weakness zone size variation (200×200, 300×300, 400×400 mm) and strength reduction magnitude (30%, 50%, 70%) characterized sensitivity to substrate defect parameters. Results quantified stress concentration factors, critical compound thickness for stress mitigation, and optimal elastic modulus range balancing load distribution against interface shear stress.

Primer performance comparison tested three systems representing prevalent European practice: silicate-based penetrating primer (System 1), epoxy resin bonding agent (System 2), and conventional cement slurry (System 3). Application occurred on concrete substrates (minimum strength 25 MPa) with controlled contamination conditions: clean reference, form oil residue simulating formwork release agents (application 0.02 g/m^2 producing visible film), and acrylic curing compound residue (0.05 g/m^2). The primer application followed manufacturer specifications with coverage rates System 1: 150 g/m^2, System 2: 300 g/m^2, System 3: 500 g/m^2 (slurry consistency). After specified cure periods (System 1: 2 hours, System 2: 12 hours, System 3: 24 hours), Type A self-leveling compound was applied at 15 mm thickness.

Bond strength evaluation via pull-off testing (EN 1542) occurred at 7, 28, and 90 days, establishing short-term development and aged performance curves. Testing employed 50 mm diameter dollies adhesively bonded to the compound surface, with failure load and mode (adhesive interface, cohesive substrate, cohesive compound) documented for each specimen. Minimum six replicates per condition ensured statistical validity. Accelerated weathering subjected primed specimens to 50 freeze-thaw cycles (EN 12371: -15°C to +20°C with 4-hour cycles, water saturation during thaw) followed by bond strength reassessment, quantifying durability under environmental stress representative of exterior or wet-area applications.

Environmental exposure testing placed additional specimens in three controlled conditions for 180 days: laboratory ambient (20°C, 50% RH), high humidity chamber (20°C, 85% RH), and wet-dry cycling (4-day wet saturation, 3-day drying at 40°C, continuous cycling). Post-exposure bond strength testing and visual documentation of degradation modes characterized primer system resistance to moisture-induced deterioration.

Statistical analysis employed analysis of variance (ANOVA) for compound performance comparison across substrate types, with Tukey post-hoc testing identifying significant pairwise differences. Regression analysis correlated substrate properties (strength, porosity, surface roughness) with bond strength outcomes. Primer system comparison utilized factorial design analyzing main effects of primer type and contamination condition plus interaction effects. Significance threshold $\alpha=0.05$ applied to all comparative testing with minimum six replicates ensuring statistical power >0.80 for detecting 20% performance differences.

Results and Discussion

Experimental characterization of self-leveling compound formulations revealed substantial performance variability across substrate types and curing conditions. Type A (polymer-modified cementitious) achieved compressive strength 32.4 MPa at 28 days on concrete substrate but only 24.8 MPa on gypsum plaster, attributed to moisture absorption differential affecting hydration kinetics. Type B (calcium sulfate-based) demonstrated an inverse pattern with superior performance on gypsum (38.7 MPa) versus concrete (28.3 MPa), reflecting chemical compatibility between calcium sulfate phases. Type C (rapid-setting) reached 28-day strength 35.6 MPa on concrete with accelerated early strength development (18.2 MPa at 24 hours), though shrinkage strain measured 620 microstrain compared to 380 microstrain for Type A. Type D (fiber-reinforced) produced intermediate compressive strength 29.8 MPa but exhibited 45% higher flexural strength (8.4 vs 5.8 MPa for Type A) and reduced shrinkage cracking severity with crack widths <0.1 mm versus 0.2-0.4 mm for unreinforced formulations.

Table 2. Self-Leveling Compound Performance on Different Substrate Types

Compound Type	Substrate	Compressive Strength 28d (MPa)	Flexural Strength (MPa)	Bond Strength (MPa)	Shrinkage Strain (με)	Elastic Modulus (GPa)
Type A (Polymer-modified)	Concrete	32.4	5.8	1.8	380	28.2
Type A	Gypsum plaster	24.8	4.9	1.2	420	22.6
Type A	Cement-lime render	28.1	5.3	1.5	410	25.4
Type B (Calcium sulfate)	Concrete	28.3	6.2	1.4	290	26.8
Type B	Gypsum plaster	38.7	7.1	1.9	310	32.4
Type C (Rapid-setting)	Concrete	35.6	6.4	1.7	620	30.1
Type D (Fiber-reinforced)	Concrete	29.8	8.4	1.6	440	27.6

Source: experimental testing results

Bond strength testing identified substrate surface condition as dominant factor controlling adhesion, overshadowing compound formulation differences. Mechanically roughened concrete (average amplitude 3 mm measured via sand patch method) achieved bond strength 1.8 MPa with Type A compound, while smooth troweled surface generated only 0.9 MPa despite identical compound application. Statistical analysis confirmed a significant interaction effect between substrate type and compound formulation ($F=8.34$, $p=0.003$), invalidating universal compound selection recommendations and establishing necessity for substrate-specific material matching. Gypsum plaster substrates exhibited bond strength ceiling 1.2–1.4 MPa regardless of preparation method, attributed to inherent cohesive weakness of gypsum matrix (tensile strength 0.8-1.2 MPa) limiting load transfer capability.

Shrinkage behavior analysis through embedded strain gauge monitoring revealed temporal patterns critical for tile installation timing. Type A compound exhibited peak shrinkage rate during 4–8 hour window post-application (85 microstrain/hour), decreasing to 12 microstrain/hour by 24 hours and stabilizing below 3 microstrain/hour after 48 hours. Type C rapid-setting formulation concentrated shrinkage within initial 2 hours (140 microstrain/hour peak rate), enabling earlier tile installation but generating higher internal stress due to constrained deformation. Residual stress estimation via ring test methodology indicated 0.8 MPa tensile stress for Type C versus 0.4 MPa for Type A at tile installation time. Fiber reinforcement in Type D reduced peak shrinkage rate 38% (52 microstrain/hour) and distributed residual strain more uniformly, decreasing risk of localized stress concentration under subsequent tile loading.

Finite element modeling quantified stress distribution in tile systems installed over substrate weakness zones, revealing load transfer mechanisms absent from uniform substrate assumptions. Distributed loading (2 kPa) over tile with a centered 300×300 mm weak substrate zone (50% strength reduction) generated maximum tile tensile stress 4.8 MPa at zone perimeter, representing stress concentration factor 2.3 compared to 2.1 MPa stress over uniform substrate. Point loading (2 kN) positioned over the weakness zone increased stress multiplication to factor 3.6, producing localized tensile stress 12.4 MPa approaching porcelain fracture threshold 15 MPa. Adhesive layer experienced maximum shear stress 1.9 MPa at weakness zone boundary under point loading, explaining debonding initiation at substrate discontinuities observed in field failures documented in literature [8][9].

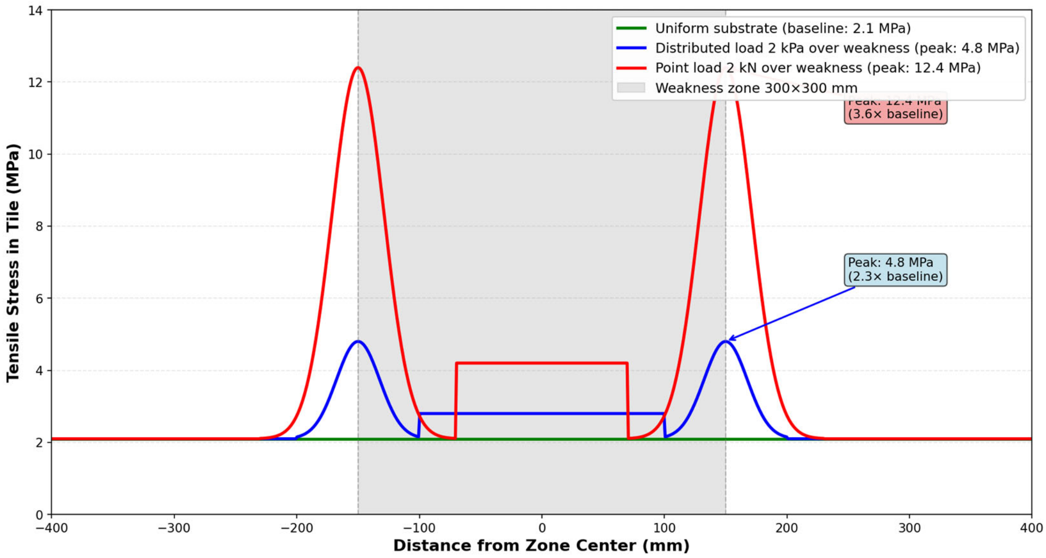

Figure 1. Tile System Stress Distribution Over Substrate Weakness Zone

Parametric analysis of self-leveling compound thickness established that a 15 mm layer over 50% strength-reduced substrate zone restored stress distribution to within 15% of uniform substrate performance. Reducing thickness to 8 mm provided only 45% stress mitigation (peak stress 8.2 MPa versus 12.4 MPa without compound), while increasing to 25 mm improved mitigation marginally to 92% (peak stress 3.9 MPa), establishing diminishing returns beyond 15–18 mm thickness range. Compound elastic modulus influenced effectiveness substantially: higher modulus materials (32 GPa) provided superior load distribution reducing peak tile stress to 4.2 MPa, but generated interface shear stress 0.9 MPa compared to 0.65 MPa for compliant compounds (24 GPa modulus). This represents 38% shear stress increase, suggesting optimal modulus exists balancing load distribution against interface stress concentration. Analysis identified optimal range 26–30 GPa for compound elastic modulus.

Weakness zone size variation demonstrated nonlinear scaling of stress concentration effects. Doubling the zone dimension from 200×200 to 400×400 mm increased peak tile stress by factor 1.6 (7.7 MPa to 12.4 MPa under point loading), indicating that larger defects generate disproportionately severe stress concentration. Strength reduction magnitude analysis confirmed exponential relationship: 30% strength reduction produced stress concentration factor 1.8, 50% reduction yielded factor 3.6, and 70% reduction generated factor 5.2, establishing critical importance of substrate strengthening when weakness exceeds 40% strength loss.

Thermal cycling simulation (5–35°C, 100 cycles representing seasonal variation) induced cumulative stress 2.4 MPa in rigidly bonded tile over compound with thermal expansion coefficient 12×10^{-6}/°C, compared to 1.6 MPa over compound with coefficient 8×10^{-6}/°C matching substrate more closely. Substrate weakness zones amplified thermal stress by factor 1.8–2.3 due to differential expansion constraint at zone boundaries, explaining seasonal cracking patterns observed in renovation installations. Compound selection minimizing thermal expansion coefficient mismatch with substrate ($\Delta\alpha < 4\times10^{-6}$/°C) reduced thermal stress accumulation below critical 3 MPa threshold for crack initiation in tile or adhesive interface.

Primer system comparison testing demonstrated substantial performance differentiation across contamination conditions. Silicate-based penetrating primer (System 1) maintained 85% bond strength on concrete with form oil contamination (0.02 g/m^2) relative to clean reference, outperforming epoxy bonding agent (System 2, 68% retention) and cement slurry (System 3, 52% retention). System 1 penetration into substrate pore structure (documented via scanning electron microscopy showing 2-4 mm penetration depth) enabled mechanical interlock beneath the contaminated surface layer. However, System 2 excelled under curing compound contamination, retaining 78% strength versus 61% for System 1 and 48% for System 3. Epoxy primer's film-forming mechanism isolated underlying concrete from surface contamination, whereas penetrating primers encountered blocked pore access. Clean substrate testing revealed minimal performance differentiation (System 1: 2.1 MPa, System 2: 2.3 MPa, System 3: 1.9 MPa), confirming that primer selection advantage manifests primarily in compromised conditions where substrate cleanliness verification proves difficult.

Table 3. Primer System Performance Under Contamination Conditions

Primer System	Clean Substrate Bond (MPa)	Form Oil Contaminated (MPa / % retention)	Curing Compound Contaminated (MPa / % retention)	Cost (€/m^2)	50-Cycle Freeze-Thaw Retention (%)
System 1 (Silicate penetrating)	2.1	1.8 / 85%	1.3 / 61%	0.80	72%
System 2 (Epoxy bonding agent)	2.3	1.6 / 68%	1.8 / 78%	2.80	81%
System 3 (Cement slurry)	1.9	1.0 / 52%	0.9 / 48%	0.40	58%

Source: experimental testing results

Freeze-thaw durability testing after 50 cycles produced bond strength retention 72% for System 1, 81% for System 2, and 58% for System 3 on concrete substrates. System 2 epoxy primer's superior environmental resistance justified 3.5× cost premium (€2.80/m^2 vs €0.80/m^2 for System 1) for exterior applications or wet environments where freeze-thaw exposure occurs. Failure mode analysis revealed that System 1 degradation occurred primarily through substrate cohesive failure (85% of failures), indicating that frost damage affected surface concrete layer rather than primer-compound interface. System 2 maintained predominantly interfacial failure mode (78%), confirming robust bond preservation. System 3 traditional cement slurry proved adequate only for high-quality substrates with minimal contamination and protected environments, explaining declining market adoption despite lowest material cost.

Environmental exposure testing over 180 days quantified moisture sensitivity differences between primer systems. High humidity exposure (85% RH) reduced System 1 bond strength 18%, System 2 by 12%, and System 3 by 31%, establishing the epoxy system as most resistant to moisture-induced degradation. Wet-dry cycling produced more severe degradation: System 1 lost 28% strength, System 2 lost 19%, and System 3 lost 47%, attributed to differential hygroscopic expansion between primer and substrate generating cyclic interface stress. These findings establish that traditional cement slurry primers (System 3) should be avoided in wet areas or high-moisture environments despite low material cost.

Integration of experimental findings with modeling results established a substrate preparation decision framework incorporating three assessment stages. Initial evaluation classifies substrate by material type (concrete, gypsum, render) and strength through rebound hammer testing (minimum acceptable: 20 MPa for concrete, 8 MPa for gypsum/render). Surface contamination assessment identifies treatments requiring removal versus primer compatibility: form oil residue compatible with System 1 penetrating primer, curing compound residue requiring System 2 epoxy primer or mechanical removal. Flatness measurement via 2-meter straightedge determines self-leveling compound necessity and optimal thickness based on deviation magnitude following formula: required thickness = 1.5× maximum deviation + 8 mm minimum, capped at 25 mm maximum for single-lift application.

Compound selection algorithm matches formulation to substrate-application combination: Type A polymer-modified for concrete substrates with standard cure time availability (48+ hours before tile installation), Type B calcium sulfate-based for gypsum-based substrates requiring maximum chemical compatibility, Type C rapid-setting for time-constrained applications where 24-hour cure acceptable despite higher shrinkage risk, Type D fiber-reinforced for weak substrates (<20 MPa concrete, <6 MPa gypsum) or heterogeneous conditions benefiting from crack control. Economic analysis established that fiber reinforcement premium (€2.40/m^2 additional material cost) proves justified when substrate strength falls below thresholds or when weakness zones exceed 15% of total area.

Economic lifecycle analysis incorporating material costs, labor requirements, and expected service life established preparation cost ranges €18–32/m^2 depending on substrate condition and selected approach. Minimal preparation approach (mechanical surface cleaning, Type A compound on adequate substrate, System 1 primer) costs €18/m^2 with projected 18-year service life generating lifecycle cost €68/m^2 including future maintenance interventions. Optimal preparation approach (substrate strengthening where required reaching minimum 20 MPa, Type D compound for weak zones, System 2 primer for contaminated areas) increases initial cost to €32/m^2 but extends service life to 28 years, reducing lifecycle cost to €52/m^2 through deferred replacement and reduced maintenance frequency.

Cost sensitivity analysis identified substrate strength as dominant lifecycle cost driver. Substrates with compressive strength <18 MPa (concrete) or <6 MPa (gypsum) generate 85–120% cost premium over service life regardless of preparation approach, attributed to accelerated degradation under tile loading. This finding establishes that when substrate strength falls below these thresholds, complete substrate replacement (removal and reconstruction) becomes an economically justified alternative to overlay preparation, with breakeven analysis showing replacement cost-effective when existing substrate strength <15 MPa and replacement achieves >25 MPa.

Conclusions

This investigation achieved its objective of establishing a quantitative substrate preparation framework for residential tile renovation through integration of experimental material characterization, computational stress analysis, and primer system evaluation under compromised surface conditions.

The research validated the hypothesis that substrate-compound compatibility exerts greater influence on system performance than compound formulation alone, with material type interactions producing 65% performance variation compared to 28% attributable to formulation differences. Chemical compatibility between calcium sulfate compounds and gypsum substrates, versus polymer-modified systems on concrete, establishes necessity for substrate-specific material matching rather than universal product selection. Substrate surface condition dominated bond development, with preparation quality overshadowing primer chemistry effects in uncontaminated applications but demonstrating critical importance under realistic renovation conditions featuring residual treatments.

Computational modeling revealed that localized substrate weakness zones generate stress concentration effects previously unquantified in tile installation literature, with magnitude scaling nonlinearly as defect severity increases. The investigation established that overlay thickness optimization follows a predictable relationship with weakness geometry, enabling rational specification replacing empirical minimum thickness defaults. Elastic modulus balancing between load distribution capability and interface stress generation identified optimal material property range for renovation applications distinct from new construction requirements.

Temporal shrinkage characterization demonstrated that installation timing windows vary substantially between formulation types, with rapid-setting systems concentrating deformation into the initial cure period creating elevated internal stress despite enabling accelerated construction schedules. Fiber reinforcement mechanisms provided crack control benefits justifying cost premium specifically in heterogeneous substrate conditions, though offering minimal advantage on uniform high-quality substrates.

Primer system performance differentiation manifested primarily under contaminated conditions representative of renovation practice, with penetrating versus film-forming mechanisms exhibiting complementary strengths across contamination types. Environmental durability testing established moisture cycling as dominant degradation mechanism for hygroscopic substrates, with traditional cementitious primers demonstrating inadequate resistance justifying transition toward polymer-modified or epoxy systems despite higher material costs.

Scientific contributions include first quantitative documentation of substrate weakness zone stress concentration factors for tile systems, validated correlation between compound shrinkage temporal patterns and installation timing requirements, contamination-specific primer performance characterization enabling evidence-based selection, and integrated decision framework synthesizing substrate assessment with material matching protocols. These advances address identified knowledge gaps in substrate heterogeneity accommodation, overlay thickness optimization beyond flatness correction, and primer selection moving from tradition-based to performance-based specification.

Practical implementation demonstrates that lifecycle cost optimization requires initial preparation investment exceeding minimal approaches, with economic modeling validating preparation quality as primary service life determinant rather than finish material selection. The research establishes substrate strength thresholds below which overlay preparation becomes economically inferior to complete substrate replacement, providing quantitative decision criteria for renovation scope determination.

Methodological limitations include experimental testing restricted to three substrate types representing prevalent but not exhaustive renovation conditions, computational modeling simplified to planar geometry neglecting edge effects and three-dimensional weakness configurations, and accelerated aging protocols potentially incomplete predictors of multi-decade field performance under variable environmental exposure. Sample sizes adequate for detecting major performance differences may lack statistical power for subtle formulation optimization.

Future research directions include extended environmental exposure beyond six-month laboratory testing to validate multi-year degradation predictions, three-dimensional finite element modeling incorporating tile installation pattern effects and complex weakness geometries, investigation of substrate strengthening alternatives (penetrating consolidants, structural overlays) comparing cost-effectiveness with replacement strategies, and field validation monitoring actual renovation projects to establish correlation between laboratory-derived preparation protocols and in-service performance outcomes.

The developed framework provides residential renovation practitioners with systematic methodology for substrate preparation specification, replacing prescriptive rules with adaptive protocols responding to actual substrate conditions. Implementation enables performance optimization within budget constraints through rational allocation between substrate improvement and finish material selection based on quantified lifecycle implications rather than initial cost minimization.

References

1. Rashid, K., Ahmad, M., Ueda, T., Deng, J., Aslam, K., Nazir, I., & Sarwar, M. A. (2020). Experimental and analytical investigation on the flexural behavior of geopolymer concrete beams reinforced with steel and FRP bars. *Journal of Building Engineering*, 30, 101272. https://doi.org/10.1016/j.jobe.2020.101272
2. Zhang, Y., Zhang, M., & Ye, G. (2020). Influence of moisture condition on chloride diffusion in partially saturated ordinary Portland cement mortar. *Materials and Structures*, 53(3), 1–14. https://doi.org/10.1617/s11527-020-01516-4
3. Dong, Z., Wu, G., Zhao, X. L., Zhu, H., & Lian, J. (2021). Bond durability of steel-FRP composite bars embedded in seawater sea-sand concrete under constant bending and shearing stress. *Construction and Building Materials*, 292, 123361. https://doi.org/10.1016/j.conbuildmat.2021.123361
4. Al-Rubaye, M., Manalo, A., Alajarmeh, O., Ferdous, W., Lokuge, W., Benmokrane, B., & Edoo, A. (2022). Flexural behaviour of concrete slabs reinforced with GFRP bars and hollow composite reinforcing systems. *Composite Structures*, 236, 111836. https://doi.org/10.1016/j.compstruct.2020.111836
5. Liu, J., Ou, G., Qiu, Q., Chen, X., Hong, J., & Xing, F. (2020). Effectiveness of saturated coral aggregate and shrinkage reducing admixture on the autogenous shrinkage of ultrahigh performance concrete. *Construction and Building Materials*, 264, 120224. https://doi.org/10.1016/j.conbuildmat.2020.120224
6. Çelik, A., Yilmaz, K., Canpolat, O., Al-Mashhadani, M. M., Aygörmez, Y., & Uysal, M. (2022). Mechanical and microstructural properties of self-compacting concretes with binary and ternary blended cementitious materials. *Journal of Building Engineering*, 56, 104746. https://doi.org/10.1016/j.jobe.2022.104746
7. Jiang, D., Li, X., Lv, Y., Zhou, M., He, C., Jiang, W., Liu, Z., & Li, C. (2020). Utilization of limestone powder and fly ash in blended cement: Rheology, strength and hydration characteristics. *Construction and Building Materials*, 232, 117228. https://doi.org/10.1016/j.conbuildmat.2019.117228

8. Zhou, Y., Guo, M., Sui, L., Xing, F., Hu, B., Huang, Z., & Yun, Y. (2021). Shear strength components of adjustable hybrid bonded CFRP shear-strengthened RC beams. *Composites Part B: Engineering*, 163, 36–51. https://doi.org/10.1016/j.compositesb.2018.11.025
9. Wang, X., Yang, Y., Yang, R., & Liu, P. (2022). Experimental analysis of bearing capacity of basalt fiber reinforced concrete short columns under axial compression. *Coatings*, 12(5), 654. https://doi.org/10.3390/coatings12050654
10. Sabău, M., Pop, I., & Oneț, T. (2021). Comparative study regarding the effect of static and dynamic loads on rheological properties of self-leveling screed mortars. *Materials*, 14(10), 2549. https://doi.org/10.3390/ma14102549
11. Li, L. G., Zhuo, H. X., Zhu, J., & Kwan, A. K. H. (2020). Packing density of mortar containing polypropylene, carbon or basalt fibres under dry and wet conditions. *Powder Technology*, 342, 433–440. https://doi.org/10.1016/j.powtec.2018.10.021
12. Zhang, P., Han, S., Ng, S., & Wang, J. (2023). Fiber-reinforced concrete with application in civil engineering. *Advances in Civil Engineering*, 2023, 1–28. https://doi.org/10.1155/2023/4142987